PAPER

Check for updates

A thin disc-shaped macrocapsule for transplantation of oxygen carrier-laden alginate hydrogel-encapsulated pancreatic islets in diabetic mice†

Nasrin Kakaei,[abc] Zhila Izadi, ![ID]*[bc] Ghobad Mohammadi,*[b] Abbas Ahmadi,*[d] Roshanak Amirian[abc] and Mohammad Raman Moloudi[e]

Pancreatic islet encapsulation has long been considered as a groundbreaking solution capable of reducing dependence on lengthy immune suppression protocols while boosting the receptivity of transplanted cells. However, its efficiency is still limited by insufficient oxygenation due to the distance to access the nearest blood supply and oxygen. During the treatment period with macrocapsules, before the effectiveness results are achieved, its negative effects will be limiting; therefore, it will affect its potential applications in the future. In our efforts to overcome existing obstacles, we encapsulated pancreatic islets into alginate hydrogel enriched by perfluorooctylbromide (PFOB) as oxygen carriers within the core of a disc-shaped macrocapsule. Physicochemical properties and biocompatibility tests were done on the designed device and then macrocapsules carrying pancreatic islets were transplanted into the peritoneal cavity of streptozotocin-induced diabetic mice and monitored for five weeks. Surprisingly, the results verified normal fast blood glucose (FBG) levels, and intraperitoneal glucose tolerance testing (IP-GTT) confirmed proper transplanted islet functionality during this time after transplantation. Our findings showcased benefits realized through implementing PFOB in alginate hydrogel by significantly increasing the oxygen supply throughout encapsulated pancreatic islets and also creating a conducive immunoprotective environment along with successful vascularization for sustained survival post-implantation.

1. Introduction

Individuals diagnosed with type 1 diabetes suffer from an auto-immune disorder that impairs the production of insulin in their bodies.[1–3] The underlying cause of this disorder lies in the self-attack on insulin-producing cells by one's own immune system. In recent years, there has been much interest in using pancreatic islet transplantation to effectively treat patients with diabetes; however, transplantation of allogeneic insulin-secreting cells do encounter host rejections due to an immediate response from their corresponding immune systems. Immunosuppressive techniques can help enhance graft survival but may come with undesired side effects. Thus, encapsulation proves to be a viable solution where a physical barrier can stop immune cell access toward transplanted cells based on MHC-mismatched transplanted cells, causing apoptosis or rejection against the donor tissue for maintaining healthy grafts long-term despite compatibility issues. Numerous approaches, including micro and macro capsules and conformal coating,[4–7] have been evaluated using various biomaterials. Currently, macrodevices are being considered due to their ability to encapsulate large volumes of pancreatic islets simultaneously,[8] easy transplantation, and retrievability for recharging or failed grafts. Macrodevices like TRAFFIC,[9] BioHub,[10,11] TheraCyte™,[12] ViaCyte®,[13,14] β-air,[11,15] and the NEED device[16] can be mentioned that have worked successfully in the clinic. A wide variety of materials were utilized in the designing and synthesizing of these devices, including alginate,[17–20] collagen,[21–23] polytetrafluoroethylene (PTFE),[24] poly(acrylonitrile-*co*-vinyl chloride) or Teflon,[16] chitosan,[25] PEG-DA,[26] polyethersulfone (PES),[27,28] and so on. PES is one of the most widely utilized in the field of medicine,[29] especially in cell transplantation in some

a Student Research Committee, Kermanshah University of Medical Sciences, Kermanshah, Iran. E-mail: nasrinkakaei331@gmail.com, roamirian@gmail.com

b Pharmaceutical Sciences Research Center, Health Institute, Kermanshah University of Medical Sciences, Kermanshah, Iran. E-mail: izadi_zh@razi.tums.ac.ir, ghobadmohammadi@yahoo.com

c USERN Office, Kermanshah University of Medical Sciences, Kermanshah, Iran

d Cellular and Molecular Research Center, Research Institute for Health Development, Kurdistan University of Medical Sciences, Sanandaj, Iran. E-mail: abbasahmady1@gmail.com

e Liver & Digestive Research Center, Research Institute for Health Development, Kurdistan University of Medical Sciences, Sanandaj, Iran. E-mail: x.moloudi@muk.ac.ir

† Electronic supplementary information (ESI) available. See DOI: https://doi.org/10.1039/d4ma00211c

treatments such as cell therapy.[30] One reason why this polymer has garnered so much attention from researchers within the field of medicine is due to its impressive versatility as well as high levels of biocompatibility. Additionally, PES exhibits strong mechanical properties combined with thermal & chemical resilience, making it an invaluable tool within certain therapies.[31,32] A potential issue pertaining to this polymer is the possibility of increased protein absorption due to its hydrophobic properties potentially leading to graft failure through subsequent fibrous tissue formation. However, surface modification strategies that incorporate hydrophilic polymers like polyethylene glycol (PEG) can address this challenge effectively.

Other studies have confirmed the use of synthetic oxygen carriers such as perfluorocarbons (PFC)[33–35] and crosslinked hemoglobin.[34] Macrocapsules provide a lot of advantages for cell enclosure and protection, but face limitations regarding insufficient oxygenation of enclosed cells due to their distance from nearby veins and oxygen sources.[8,36] Up until the present, numerous attempts have been made to focus on this problem during the early post-transplant period to supply oxygen, including pre-vascularized deviceless sites,[37] proangiogenic factors concomitant with transplanted islets,[38,39] and in situ generation of oxygen with the hydration of solid peroxide accompanied by islets.[40,41] PFCs have the ability to dissolve diverse gases like CO_2, NO and O_2 in substantial quantities that are useful in certain situations. Unlike hemoglobin's relationship between the amount of the gas present and its partial pressure that has a sigmoidal curve, PFC emulsions give a linear association enabling easy tracking or monitoring of supplementary oxygen levels delivered during transplantation of allogeneic insulin-secreting cells being both biologically compatible yet chemically inert. This has enormous practical implications in improving outcomes following cellular transplants. One key derivative worth considering within this group is perfluorooctylbromide (PFOB) based on the wealth of documented research,[42] and perfluorotributylamine (PFTBA)[43] and perfluorodecalin (PFD)[44] have been evaluated for supplying oxygen to bioartificial tissues.[45–48] Here, we report the integration of an oxygenation and immunoprotection strategy to improve survival and function of transplanted pancreatic islets using the design of surface-modified thin disc-shaped microcapsules with PEG, which is fabricated for encapsulation of pancreatic islets embedded into PFOB nanoemulsion-enriched hydrogel. Once the macrodevice was implanted in the peritoneal cavity of streptozotocin-induced diabetic mice without immunosuppressant therapy, it led to normoglycemia over an extended period and noteworthy survival rates in diabetic mice. In particular, we were able to recover the pancreatic islet-carrying device five weeks after transplantation without any adhesion to the surrounding fibrosis tissues.

2. Materials and methods

2.1. Materials

Sodium bicarbonate, calcium chloride, bovine serum albumin (BSA), polyethylene glycol (PEG; MW = 600 Da), fluorescein diacetate (FDA), propidium iodide (PI), poloxamer 188, perfluorooctylbromide (PFOB), streptozotocin, polyvinylpyrrolidone (PVP, MW = 40 000 g mol^{-1}), n-methyl-2-pyrrolidone and collagenase were purchased from Sigma Aldrich. Hank's buffered saline solution (HBSS), Ficoll, and phosphate-buffered saline (PBS) were purchased from Gibco. (RPMI)-1640 medium and penicillin/streptomycin were purchased from Invitrogen. Sodium alginate was purchased from NovaMatrix. PES, (MW = 58 000 g mol^{-1}) was purchased from BASF (Co., Germany).

2.2. Rat pancreatic islet isolation: purity, viability and functionality tests

Islets were separated using the Royan Institute procedure.[49] Male Wistar rats weighing 250–300 g and aged 8–10 weeks were sedated with ketamine and xylazine. We dissolved 1 mg mL^{-1} collagenase enzyme in HBSS (1×) and perfused it via the common bile duct. After separating the pancreas from the other tissues, the pancreas were enzymatically digested in a 37 °C water bath. Centrifugation with a focal density gradient was used to separate islets from exocrine tissue. The islets were then cultivated for 24 h in full RPMI-1640 media (FBS 10%, pen/strep 1%, and L-glutamate 1%). The islet yield was investigated using dithizone staining. The collected data were transformed into a standard number of islet equivalents (IEQ), and the standardized islet diameter was 150 μm.[50] In order to evaluate the quality of isolated islets before encapsulation and transplantation, we assessed viability and functionality of these islets on fresh islets and 24 h post-isolation with live/dead imaging for viability and the glucose-stimulated insulin secretion (GSIS) assay for functionality based on our previous works.[20,50] Briefly, the FDA/PI staining kit was used to assess the vitality of isolated pancreatic islets. The isolated islets in 480 μL DPBS were stained in the dark with 10 μL DPBS that contained 0.46 μM FDA and 14.43 μM PI and immediately assessed by fluorescence microscopy (Nikon TIE, Japan). The GSIS assay was performed to evaluate the function of the islets. The islets were incubated within the cell inserts (Millipore) in triplicate in a 24-well plate (20 islets/well) and challenged with either 2.8 mM or 28 mM glucose for 1 h in Krebs-bicarbonate buffer (KRBB) comprised of 99 mM NaCl, 5 mM KCl, 1.2 mM KH_2PO_4, 1.2 mM $MgSO_4$, 2.6 mM $CaCl_2$, 26 mM $NaHCO_3$, and 0.2 wt% BSA, followed by washing with glucose solution. The amount of insulin secreted into the low-glucose and high-glucose solutions was measured with a rat insulin enzyme-linked immunosorbent assay (ELISA) kit (Thermo Fisher). The stimulation index (SI), or the ratio of normalized insulin secreted in the high glucose group to that of the low glucose group, was calculated for both islet samples.

2.3. Fabrication and surface modification of thin disc-shaped macrocapsules

Briefly, polyethersulfone (PES 18%) (optimum) (3.6 g. ultrasound, E6020P, molecular weight of 58 000 g mol^{-1},) and polyvinylpyrrolidone (0.02 g. MW = 40 000 g mol^{-1}, Sigma Aldrich) were dissolved in N-methylpyrrolidone (NMP) (across organic) solvent. This polymer solution was stirred overnight at 25 °C on a shaker incubator to obtain a clear and homogenous

solution. Then, a thin membrane was fabricated by the phase inversion method.[51]

The surface of the thin-disc membranes was modified using PEG (MW = 600 Da). After immersing the thin membranes in the PEG solution for 5 minutes, they were subjected to an 18-watt UV lamp[52] for 10 minutes before being activated by UV light. Then, the membrane was submerged in the solution for another 40 minutes to allow the PEG to react and finally, the thin membranes were rinsed three times with distilled water before being dried and kept for the following procedure.

2.4. Fabrication of PFOB-laden alginate hydrogels

For the primary protection of pancreatic islets, they were encapsulated in PFOB-laden alginate hydrogel. Briefly, an alginate solution with a final concentration of 1% sodium alginate dissolved in deionized water under stirring for 24 h was prepared. Then, to prepare the PFOB nanoemulsion, PFOB oxygen carrier and poloxamer 188 with final concentrations of 10% and 1%, respectively, were prepared using a probe sonicator (Thermo Fisher Aquasonic 75HT sonicator) and related characterization tests were done to evaluate their size, zeta potential and polydispersity properties. Following this, the PFOB nanoemulsion was added to the alginate solution in a ratio of 1 to 4. Subsequently, by adding calcium chloride (100 mM) solution under stirrer conditions, PFOB-laden alginate hydrogel was formed. Swelling and biocompatibility properties were evaluated on the alginate hydrogel.

2.5. Characterization of the macrocapsule

2.5.1. Scanning electron microscopy (SEM).
Scanning electron microscopy was used to examine the morphological changes of the produced unmodified thin membranes and changed thin membrane. Thin-membranes were submerged in liquid nitrogen for 1 minute at room temperature and then fractured to increase the resolution of the cross-sectional picture. Members' cross-sections and surfaces are coated with a thin coating of gold/palladium to reduce electrical charge.

2.5.2. Attenuated total reflectance (ATR)-Fourier transform infrared (FT-IR) spectroscopy.
In order to assess the surface modification of the thin membranes, FT-IR and FTIR-ATR analyses were performed. The evaluation with the FTIR-ATR spectroscopy model (Galaxy Series 5000) and the FT-IR spectroscopy model (Irprestige-21, Shimadzu) was performed in the range of wavenumber 600–4000 cm^{-1}.

2.5.3. Contact angle measurement.
The hydrophilicity qualities of the modified and unmodified thin membranes are measured using the sessile drop technique by measuring the contact angle between the thin-membrane surface and the water drop (5–25 μL). Deionized water was injected from a needle tip into the surface of a thin membrane with dimensions of 1 × 5 cm^2 at three distinct places at room temperature. After 10 seconds, a digital camera captured a magnified picture of the descent. Image J software was used to automatically measure the contact angles.

2.5.4. Mechanical stability.
The mechanical properties, including tensile strength and elongation, of modified and unmodified thin membranes were determined by a tensile test.

Thin membranes with dimensions of 1 × 5 cm^2 were located vertically between two clamps. The measurements for the tensile strength and elongation of the thin membranes were set at a constant elongation rate of 1 mm per minute at room temperature. Each sample was repeated three times, and the average was reported.

2.5.5. Protein absorption study.
The Ponceau S staining technique was used to assess the protein absorption capabilities of the modified and unmodified thin membranes. Thin membranes were submerged in a protein solution containing serum albumin (BSA) at 10 mg mL^{-1} concentration for 1 h before being immersed in 2% SDS solution in a shaker incubator for 30 minutes. Following that, drops of Ponceau S 5% dyed solution were put over the thin membrane and rinsed three times with distilled water after 1 minute. Color differences were found in the changed and unmodified thin membranes, with each sample repeated thrice.

2.6. Swelling study

To study the swelling behavior of alginate hydrogel, the hydrogel was first dried in a vacuum oven at 50 °C until a constant weight of the gel was obtained. This dry sample was immersed in deionized water at room temperature and evaluated for the change in weight of the hydrogel at different time intervals. This examination of weight changes continues until a constant weight of the gel is obtained. The degree of swelling can be calculated with the following equation:

$$\% \text{ DS} = (W_2 - W_1)/W_1 \times 100 \qquad (1)$$

In this equation, DS is the degree of swelling in percent, and W_1 and W_2 are the weights of the sample before and after swelling.

2.7. Dynamic light scattering (DLS)

The hydrodynamic diameters, zeta potentials, and polydispersity of the PFOB emulsion were determined by dynamic light scattering (DLS) with a Malvern Nano ZS Zetasizer (Malvern Instruments Ltd, Malvern, UK) at room temperature. For preparation, the PFOB emulsion was sonicated for 30 minutes with a probe sonicator (Hielscher, UP 100 H).

2.8. Assessment of oxygen release from PFOB-laden alginate hydrogel

Assessment of oxygen release from PFOB-laden alginate hydrogel was performed by two methods. Method 1: firstly, 100 μL of Alg/PFOB was added to 1 mL of degassed water, and then at intervals of 0, 15, 30, 60, 90, and 120 minutes, the oxygen gas pressure was measured by an arterial blood gas (ABG) device (Techno medica). At the same time, one sample (dd H_2O) was measured as a control. The experiment was performed at ambient temperature and repeated three times, and the average was reported.

Method 2: by using a fluorescence-based oxygen probe, $[Ru(dpp)_3]Cl_2$, oxygen release was detected. Firstly, tubes containing 1 mL of $[Ru(dpp)_3]Cl_2$ (0.1 μM in PBS) solution were

prepared; one vial contained 0.3 mg Alg, and another contained 0.3 mg Alg and 0.3 mg PFOB. To prevent the free air exchange, the vials were capped. After reaction, the emission spectrum of $[Ru(dpp)_3]Cl_2$ was read with an excitation of 455 nm.

2.9. *In vitro* biocompatibility assessments

2.9.1. Blood compatibility. For this purpose, 2 mL of human blood, which was collected in a tube containing EDTA, was centrifuged for 2 minutes at a speed of 13 000 rpm to separate the red blood cells from the plasma. Then the red blood cells were washed three times with PBS buffer. After the last wash, red blood cells were divided into separate microtubes, so that 100 million red blood cells were poured into each microtube. Then, the final volume in each of the samples was adjusted to 1 mL using PBS (pH = 7.4) and incubated with 0.5×0.5 cm of thin membrane for 1 h at 37 °C at a speed of 50 cycles per min. Then, the tubes were centrifuged for 5 minutes at a speed of 13 000 rpm, and finally, the absorbance of the supernatant solution was measured at a wavelength of 540 nm. In this experiment, red blood cells treated with 1% Triton solution and PBS buffer are considered positive and negative control groups, respectively.

2.9.2. Cell compatibility. The thin disc-shaped macrocapsule was sterilized by UV, immersed in DMEM medium, and incubated at 37 °C for 2 h. In the next step, the medium was removed, mouse insulinoma (MIN6) cells as pseudo-islets with a density of 1×10^4 cells per cm^2 in culture medium (DMEM, FBS 10%, pen/strep 1%) were cultured on the surface of the thin membranes, and then cell viability was evaluated after 1, 3, and 7 days by the MTT method. The wells containing cells without any treatment were considered as a control group. MTT reagent was added and incubated at 37 °C for 4 h in the dark. Accumulated formazan was dissolved by adding DMSO for 30 minutes. Finally, the absorbance of the solutions was read at 570 nm. The cell compatibility of the alginate hydrogel with or without PFOB was evaluated by MIN6 cells as mimic cells for pancreatic islets by the MTT method under the same conditions at 2 and 5 days.

MIN6 cells were used to evaluate *in vitro* cell compatibility of PFOB-laden alginate hydrogel. Therefore, MIN6 cells were cultured in the DMEM containing 15% FBS, 100 IU mL^{-1} penicillin, 100 μg mL^{-1} streptomycin at 37 °C under 5% CO$_2$. Prior to immersing cells into PFOB-laden alginate hydrogel, the cells were detached from the cell culture plates with a 0.25% trypsin-EDTA solution and resuspended in DMEM at a cell density of 5×10^5. Then, 5×10^5 cells add to a microtube containing 100 μL of the solution of PFOB-laden alginate hydrogel and a crosslinking process was done by CaCl$_2$ solution. The mixture was incubated at 37 °C for 30 minutes and then fresh DMEM/15% FBS was added to the well containing MIN6 cell-embedded PFOB-laden hydrogel followed by the cell viability assay.

2.10. Diabetes induction in mice

Male C57BL/6 mice were purchased from Razi (Tehran, Iran). Two weeks after adapting to the nutritional conditions, they were randomly divided into control and diabetic groups. Type 1 diabetes was induced by multiple doses injecting streptozotocin (STZ, 50 mg kg^{-1} in 0.1 mmol L^{-1} citric acid buffer, pH = 4.5) in the peritoneal cavity of C57 mice with a weight range between 17–22 g and an age of 6–8 weeks for 5 consecutive days. An equal amount of sodium citrate buffer solution was injected into the mice of the control group. The mice fasted for 6 h before injection, and their FBG level was determined before injection. After the last dose of STZ, FBG levels were measured every other day, up to two weeks until their FBG was more than 250 mg dL^{-1}, and they were considered diabetic.

2.11. Implantation

In the implantation phase, the assembling of macrocapsules was done by the insertion of pancreatic islet-PFOB-laden alginate hydrogel into two thin disc-shaped layers and then, the edges of the two disk-shaped layers were bonded with biological glue.

Diabetic mice were randomly divided into four groups: (i) untreated diabetic mice; (ii) free-islet; (iii) macrocapsule (islet-PFOB-hydrogel); and (iv) macrocapsule (islet-hydrogel), and the devices were implanted into the peritoneal cavity of all diabetic mice after 24 h fasting (the peritoneal cavity is a suitable graft site due to the macrocapsule's large size and easier vascularization). The last 3 groups were transplanted with a minimal mass of islets (500 IEQ). Xenograft function was assessed by monitoring the fasting blood glucose (FBG) levels from each recipient during five weeks post-transplantation, and immunohistochemical staining was performed on the retrieved macrocapsules on the last day of following up. All animal experiments were carried out according to the NIH Guidelines for the Care and Use of Laboratory Animals (NIH Publication No. 85e23, revised 2010) after approval from the Royan Institute.

2.11.1. Blood glucose monitoring and intraperitoneal glucose tolerance test. FBG levels in mice were evaluated every 5 days for 35 days after transplanting using a Care Sens glucometer and snipping blood from the tail vein. Intraperitoneal glucose tolerance tests were done in all groups 20–35 days following implantation. The mice were fasted for 6 h before the injection, and blood glucose was monitored using a glucometer at time intervals of 0, 15, 30, 60, and 120 minutes following the intraperitoneal injection of 2 g kg^{-1}.

2.11.2. Histological analysis and immunostaining. The retrieved macrodevices were immediately preserved in 4% paraformaldehyde for 48 h. The specimen was then fixed in paraffin and sectioned at a thickness of 4 μm. The sections were deparaffinized with xylene before being rehydrated in serially graded ethanol. After that, the slices were stained with hematoxylin and eosin (H&E) and Masson's trichrome (MT) stains.[40] The development of endothelial cells and collagen fibers was observed using an Olympus inverted microscope on histology slides.

2.12. Statistical analysis

Data points were expressed as the mean $\pm$ SD. GraphPad Prism (9) and SPSS (22) software were used for data analysis. Statistical analysis was performed by independent *t*-tests, one-way ANOVA, and repeated measures. $P < 0.05$ was used as the significance level.

3. Results

3.1. Fabricated membrane

A schematic figure of the thin membrane of PES and its modification process by PEG is illustrated in Fig. 1A. The FT-IR and ATR-FTIR spectra of the modified and unmodified thin membranes are shown in Fig. 1B. For the fabrication and optimization of the membranes, different percentages of PES, PVA, and PEG were evaluated, as shown in S1A and B (ESI†). Based on the results (Fig. 1B), most of the peaks and functional groups are the same in both spectra. Peaks related to the benzene structure, the ether group, and the sulfone structure are observed in both spectra. The three peaks between 1400 and 1600 cm^{-1} indicate C=C aromatic stretching vibrations, and the peak at 3085 cm^{-1} corresponds to C–H stretching of the benzene ring. The peaks related to the C–O–C ether stretching band were observed at 1240–1316 cm^{-1} wavenumbers; also, the peak in the range of 1104–1153 cm^{-1} confirms the functional group of O=S=O. But after modification of the thin membrane, in addition to the mentioned peaks, other peaks have appeared in the wavenumbers 2200–2800 cm^{-1} and 3200–3600 cm^{-1}, which are related to the hydroxyl (–OH) and alkyl (CH$_2$) groups, respectively.

SEM images of the thin membrane's surface and cross section were obtained to evaluate the influence of surface modification on the morphology of the thin membranes. The surface images of the thin membranes before and after modification are smooth and homogeneous, as shown in Fig. 1C, and their morphology is identical. The porous nature of the thin membranes is seen in cross-sectional photographs. As a result, the modification technique had no negative impact on the morphology or porosity of the thin membranes. The pore size has not altered much after the adjustment. More results related to other percentages of microcapsule components are provided in S2 (ESI†).

The contact angle measurement results showed that by modifying the surface of the synthesized thin membranes, the contact angle decreased from 51° to 30.5°, proving the efficacy of PEG(OH)$_2$ grafting with UV on the PES thin membrane and confirming the change from hydrophobicity to hydrophilicity (Fig. 1D and Fig. S3, ESI†).

The mechanical strength, the thermal stability and the chemical resistance are the advantages of the PES thin membrane. Table 1 in ESI† (S4) shows the influence of surface modification on the mechanical characteristics of the thin membranes. These findings demonstrated that following alteration, the tensile stress at break and strain at break were reduced. Despite this, it has strong mechanical and chemical resistance. The protein absorption properties of the membranes depict the influence of surface modification on the thin membranes using Ponceau S staining. The chemistry of the surface has transitioned to hydrophilicity based on contact angle data, and the color intensity, which is an indicator of protein absorption on the surface of the thin membranes, has reduced dramatically (S5, ESI†).

Fig. 2A presents the results of the cellular biocompatibility test for the membrane. The data indicated that the membrane
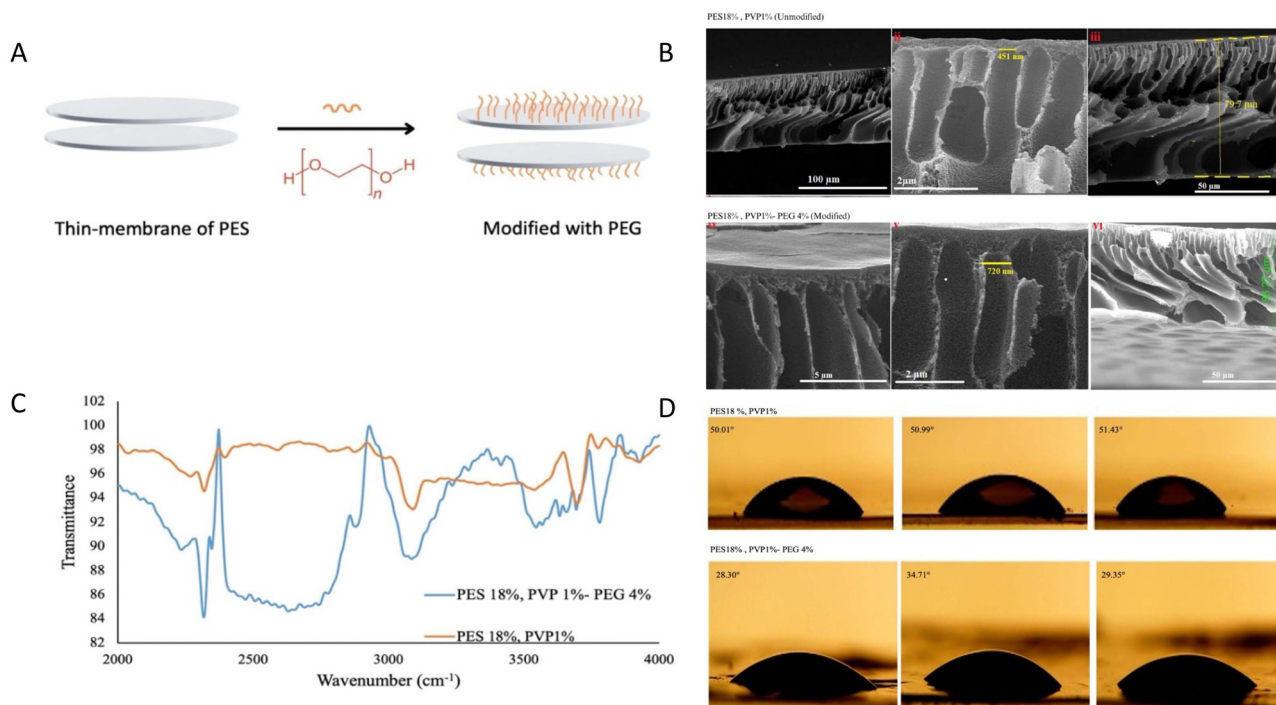
Fig. 1 Chemical identification of the PES thin membrane before and after modification. (A) A schematic figure of the thin-membrane of PES and its modification process. (B) Comparison of FT-IR and FTIR-ATR spectra of modified and unmodified PES thin membranes, which show common functional groups in both spectra. (C) Cross-sectional and surface SEM images of unmodified and modified thin membranes. (D) Comparison of the contact angles before and after surface modification. The contact angle is reduced in the modified thin membrane.

exhibits high cell compatibility, as evidenced by the high cell viability observed. The design of the membrane requires it to be implanted for an extended period of time and in contact with bodily fluids. As such, assessing blood compatibility is crucial. The amount of hemolysis observed in all modified and unmodified thin membranes was less than 1%, in comparison to the positive control groups, which showed 100% hemolysis (Fig. 2B).

3.2. PFOB-laden alginate hydrogel stability and biocompatibility *in vitro*

The alginate hydrogel is supplemented with perfluorooctylbromide (PFOB), which is demonstrated in Fig. 3A. Alginate polymers have the ability to absorb water or physiological body fluids and expand. As shown in Fig. 3B, the manufactured hydrogel exhibits this swelling behavior. Based on the degradation analysis, the hydrogel exhibits an optimal rate of degradation, with its swelling percentage exceeding 900% after immersion in water for 40 h. Changes in the hydrogel's elongation over time suggest chemical alterations. The maximum mass expansion of the

Fig. 2 Biocompatibility study of membranes before and after modification. (A) The results of the MTT assay after culture of MIN6 cells on the surface of thin membranes in three different time periods, not only did it show no toxicity, but cell proliferation was also observed. Data points are presented as mean ± SD for a minimum of 3 independent measurements at each time point, $n = 6$. ($p \leq 0.05$, **: $p \leq 0.01$, ***: $p \leq 0.001$). (B) Comparison of the percentage hemolysis in both modified and unmodified thin membranes with the control group, which is less than 1% in the membranes.

alginate hydrogel was observed at 170 h. The results indicated that the amount of swelling increases up to 170 h before decreasing. The results of the particle size and zeta potential distribution spectrum for the optimal PFOB emulsion are illustrated in S6 (ESI†). The average diameter of the PFOB nanoparticles at ambient temperature was measured to be 136 nm using dynamic light scattering (DLS) techniques. The zeta potential and polydispersity index (PDI) values are −108 mV and 0.29, indicating a restricted size distribution.

Using two distinct methodologies, the oxygen release profile of the PFOB-containing alginate hydrogel was measured. According to the data presented in Fig. 3C, the amount of oxygen released in the PFOB-laden alginate hydrogel group increased from 80 mmHg to 170 mmHg over a period of 120 minutes. This represents a significant difference compared to the control group, which showed no increase in pO_2 levels during the same time period. As illustrated in Fig. 3D, a fluorescent probe was employed to measure the fluorescence emission spectrum of the alginate hydrogel and PFOB-loaded alginate hydrogel. Due to the release of oxygen from the PFOB, the fluorescence emission spectrum of the Alg-PFOB groups is 41 nm shorter than that of the Alg groups around 610 nm. The viability of MIN6 cells in an alginate hydrogel that contained PFOB was evaluated using the MTT assay. To avoid the need for animal sacrifice for islet isolation, MIN6 cells, which exhibit islet-like functionality, were utilized in the MTT assay. The data indicate that PFOB-containing alginate exhibits high cell compatibility, as evidenced by the high cell viability observed (Fig. 3E).

3.3. Quality control test on the isolated pancreatic islets before transplantation

In order to ensure the quality of isolated pancreatic islets (Fig. 4A), the viability and functionality of the islets were evaluated before encapsulation and transplantation. Light microscopy images show the appearance and quality of isolated pancreatic islets (Fig. 4B and C). Glucose-stimulated insulin secretion, a stringent test of islet functionality, was assessed after a 24 h incubation of islets in a high glucose medium. The islets 24 h post-isolation showed a stimulation index greater than 1.5 that was significantly higher than the value for fresh islets on day 0 (1.54 *vs.* 0.63, $p < 0.01$, Fig. 4D). In addition, the live/dead assay showed that incubation of islets for 24 h post-isolation can be the right time to repair the effects of the isolation process on the islet cells, and it is the ideal time to prepare for their transplantation (Fig. 4E and F).

3.4. Effectiveness of implantation of encapsulated pancreatic islets

A flow chart of the experimental design is shown in Fig. 5A. The results of the animal phase showed that implanted membranes containing islets were capsulated into PFOB-enriched alginate, and the FBG level remained in the normoglycemia range until 35 days post-transplantation. However, this group showed a significant difference from the other groups. Healthy mice and diabetic mice served as positive and negative controls, respectively (Fig. 5B). To assess the glucose responsiveness of the islets
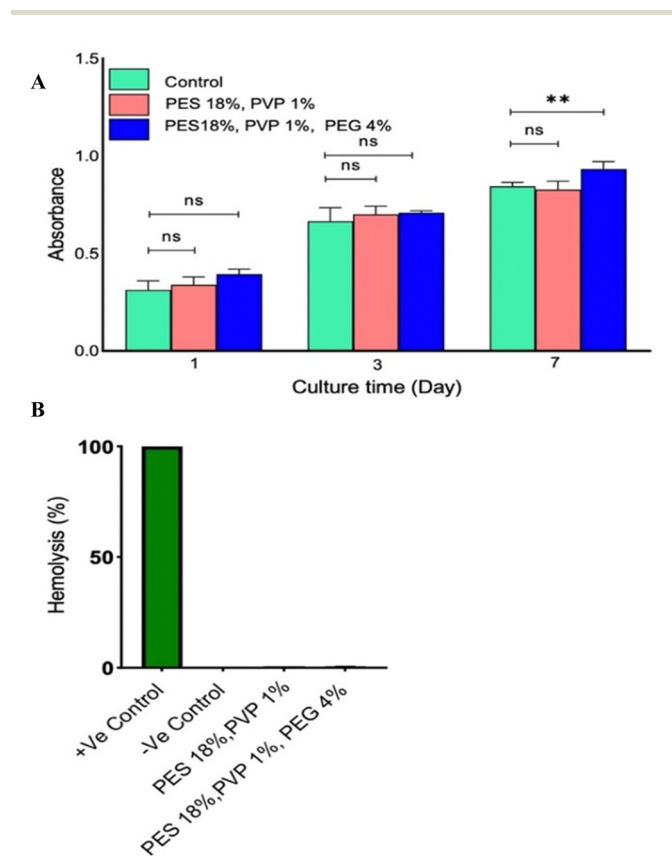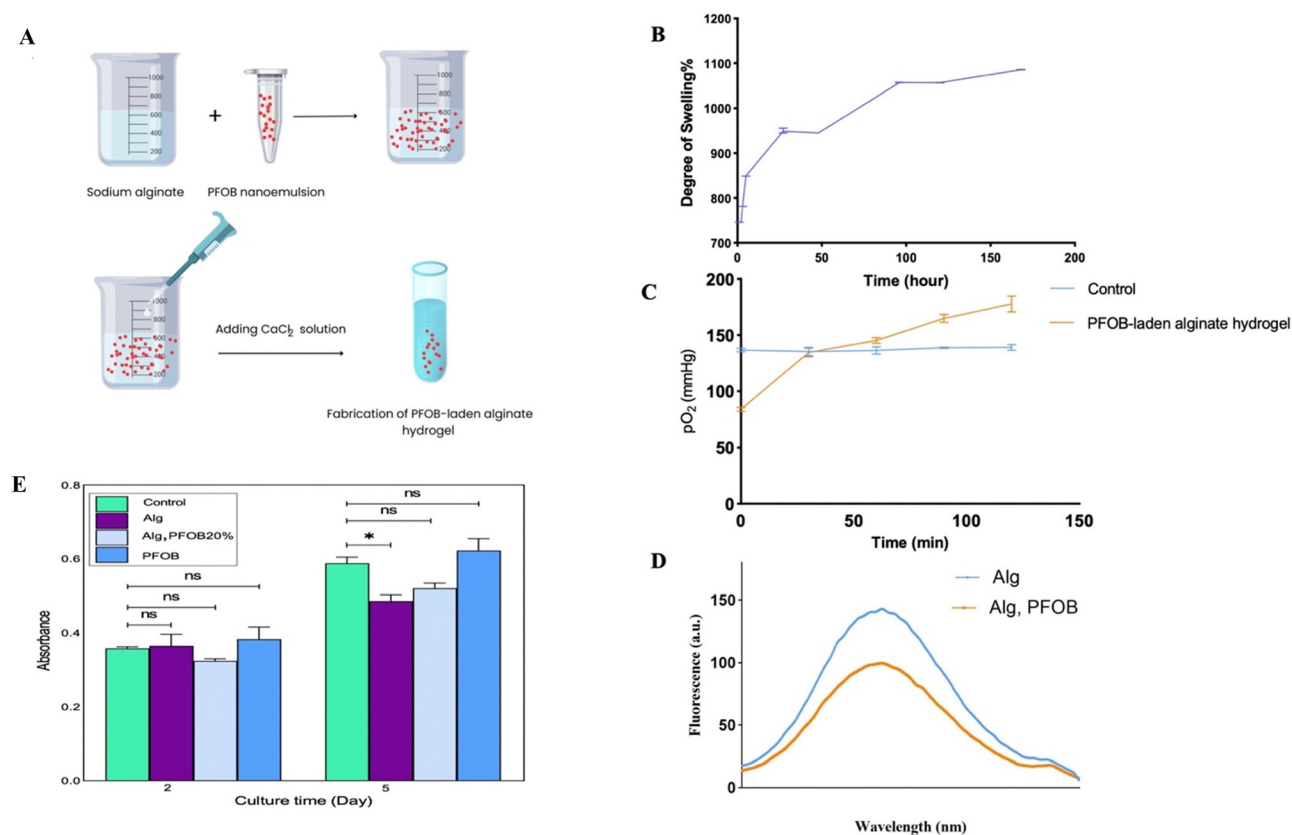
Fig. 3 Study of the swelling property of alginate hydrogel, oxygen release profile of PFOB emulsion with two different methods, and the biocompatibility study. (A) A schematic illustration of PFOB-enriched alginate hydrogel. (B) The swelling percentages of the alginate hydrogel over time. The highest swelling percentage was at 170 h after the incubation. (C) Results of oxygen release of the PFOB nanoemulsion at different times by the ABG device. The results show significant differences in the PFOB group compared to the control group. (D) The evaluation of oxygen release from the PFOB nanoemulsion by the fluorescence method: by $[Ru(dpp)_3]Cl_2$ assay, there was a significant decrease in $[Ru(dpp)_3]Cl_2$ fluorescence at 610 nm in the diagram of PFOB-laden alginate hydrogel. (E) The results of biocompatibility *in vitro* after culturing MIN6 cells into PFOB-laden alginate hydrogel, and incubating cells with PFOB, and alginate in both incubation times showed high cell compatibility. Data points are presented as mean $\pm$ SD for a minimum of 3 independent measurements at each time point. ($p \leq 0.05$, **: $p \leq 0.01$, ***: $p \leq 0.001$).

transplanted into each group, we conducted an intraperitoneal glucose tolerance test (IP-GTT) when the FBG level was at its minimum. Fig. 4C shows the FBG levels for all groups. The FBG level of all groups increased 20 minutes after the injection, but the groups that received the membrane (islet/PFOB/Alg) followed a similar decreasing trend as the healthy group.

In order to evaluate the effect of modification on angiogenesis and the possibility of fibrotic tissue of the implanted membranes, immunohistochemistry staining was performed. So, the modified and unmodified membranes were retrieved five weeks post-transplantation. The modified membrane was easily retrieved, but the unmodified membrane was forming severe fibrosis. The images of H&E and MT staining are depicted in Fig. 6. According to the results of the H&E-stained images, the modified membrane after retrieval (Fig. 6A and B) showed a high density of vascular tissue in comparison to the unmodified one, which showed very limited and invisible vascularization. In confirmation of these results, the formation of collagen fibers marked by a blue color was clearly observed in MT staining images of unmodified membranes (Fig. 6D), while no such collagen fibers were visible in the modified

membrane (Fig. 6C). Also, the density of blood vessels is quantitatively presented in the modified membranes in Fig. 6E.

4. Discussion

Transplanting cells and tissues presents an immense challenge when it comes to maintaining adequate oxygen supply in scaffolds during the post-transplant stage. The long-term viability of transplanted cells can only be ensured when this obstacle has been overcome.[40,53–55] The dense vascular network found in pancreatic tissue allows blood circulation to provide sufficient levels of oxygen required by pancreatic islets, which easily suffer from hypoxic conditions, as various studies have shown.[56] However, achieving vascularization within the implanted scaffold takes time, so making readily available oxygen is crucial for maintaining the metabolic demands and physiological functions of native islet cells.[54,57,58] A minimum pressure level of 40 mmHg should always be maintained within the pancreas regarding oxygen, as insufficient access poses one of the main reasons behind graft failure.[59] A macrocapsule that
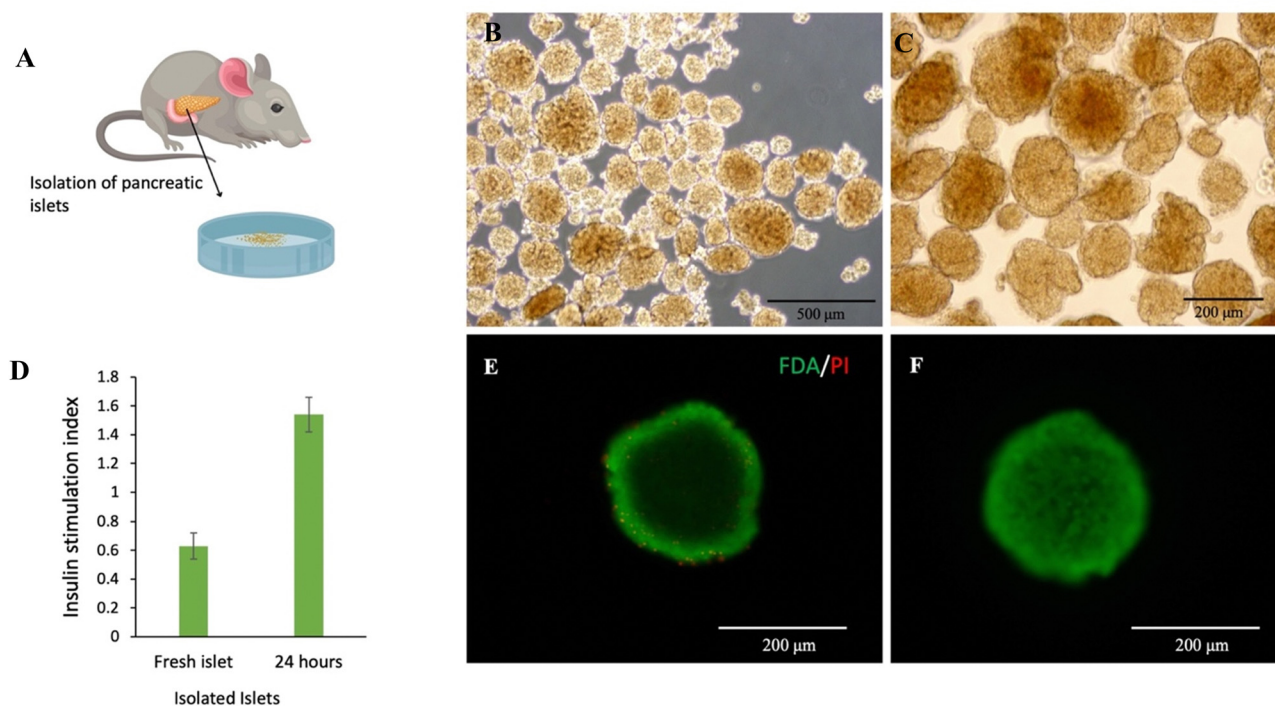
Fig. 4 The results of quality control tests on isolated pancreatic islets before transplantation. (A) A schematic illustration of isolated pancreatic islets. (B) and (C) Light microscopy images show the appearance quality of isolated pancreatic islets. (D) Glucose-stimulated insulin secretion, a stringent test of islet functionality, was assessed after a 24 h incubation of islets in a high glucose medium. The islets in 24 h post-isolation showed a stimulation index greater than 1.5 that was significantly higher than the value for fresh islets on day 0 (1.54 $vs.$ 0.63, $p < 0.01$) (E) and (F). Fluorescent microscope images of the pancreatic islets with FDA/PI. Pancreatic islets after isolation (fresh islets) and 24 h post-isolation. Scale bar: 200 μm.

contains alginate hydrogel with PFOB was designed by our study for pancreatic islet transplantation, with the main purpose of providing oxygen post-transplantation. By using a PVP pore maker, the phase separation method can produce a porous thin membrane adjustable pore size. Using PEG 600 modifications, we solved the problem of the capsule surface being very hydrophobic. This problem and the increased risk of fibrotic formation resulted from using 1% PVP as a pore-maker.

Skrzypek K. $et\ al.$ used micropatterns and 5% PVP with the one-step PSμM method. Their device did not need modifications and was hydrophilic, but they only tested it $in\ vitro$. We had to use a modified method because our PVP percentages were different.[27]

It is worth noting that despite the use of a low percentage of PVP causing hydrophobicity in the thin membrane, it offers an excellent advantage by facilitating pore creation smaller than 1 μm–a key objective while designing macrocapsules. Smaller pores aid in the transport of minute molecules and prevent immune cells from entering, a pivotal factor contributing to graft success. J. A. Prince $et\ al.$ did research on PES hollow fibers and used thermal grafting with silver nanoparticles and PEG, which lowered the contact angle from 62° to 15.5°.[60]

Our research has demonstrated that modifying PES membrane surfaces has led to reduced contact angles. Nevertheless, alternative methods and materials have surpassed our work in producing even greater reductions. A noteworthy example comes from recent investigations that leveraged poly(ether glycol) methyl ether methacrylate (PEGMA) under mild conditions for modifying membrane surfaces. With increasing PEGMA proportions, these surfaces saw drops in their contact angles, going from 63° down to 46°.[61]

Reducing contact angles and altering surfaces from being hydrophobic to hydrophilic occurs when using PEG modifications on surfaces. The extent of reduction depends on factors such as the amount of PEG polymer used and the technique employed during modification processes. Blood cell destruction and thrombosis causing kidney failure happen if macrocapsules interact too closely with these cells; hence, biomaterials must not have features contributing to protein uptake by blood cells; hemolysis less than 2% ensures optimal hemocompatibility, as our results show.[11,62,63]

Another important criterion for the success of transplanted macrocapsules was the inhibition of blood protein absorption on the macrocapsule's surface. So, adequate nutrition transmission to encapsulated cells and excretion is connected to protein absorption; under these circumstances, glucose diffusion into the macrocapsule and insulin release are readily achieved.

Another feature of the developed macrocapsule that was tested was its biocompatibility. In comparison to the control group, the findings demonstrated no toxicity. Also, surface modification of the macrocapsule improved the vitality of the seeded cells, which is consistent with earlier PES research.[64,65]

Swelling was employed to test the stability of the alginate hydrogel used in the macrocapsule reservoir. The rate of
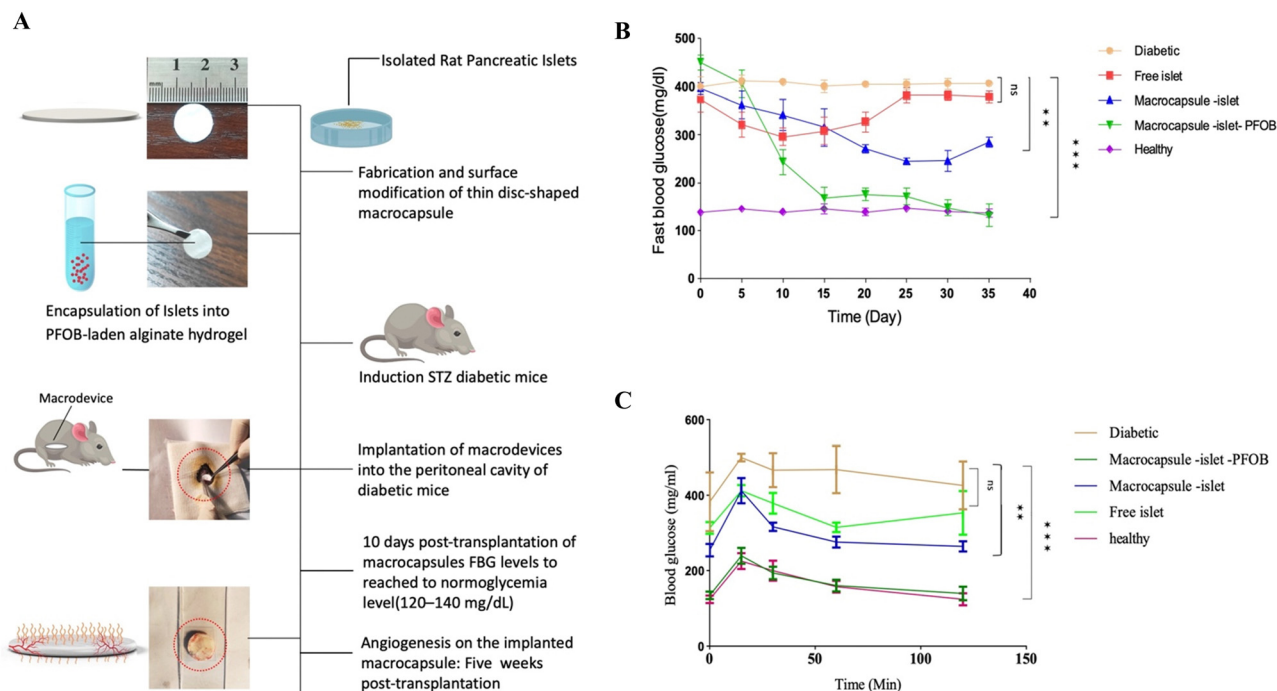
Fig. 5 *In vivo* evaluation of islet encapsulation in the treatment of type 1 diabetes and retrieval of the macrocapsule. (A) Experimental flow diagram. Procedure for fabrication of the macrocapsule, culture of isolated islets, PFOB-containing alginate hydrogel and encapsulation of islets in the hydrogel and macrocapsule, diabetic induction, and its implantation. (B) Fasting blood glucose (FBG) levels of diabetic C57BL/6 mice transplanted with 500 islets equivalent (IEQ) to groups in: macrocapsule-islet ($n = 6$), macrocapsule-islet-PFOB ($n = 6$), and free islet ($n = 6$). A group of mice that received the macrocapsule-islet-PFOB showed a lower FBG level compared to the free islet and microcapsule-islet group ($P < 0.005$). Data are represented as mean ± SD. (C) Intraperitoneal glucose tolerance test (IP-GTT) for all groups, post transplantation. The macrocapsule-islet-PFOB group, the same as the healthy group, displayed the ideal response in the GTT test. Data points are presented as mean ± SD for a minimum of 3 independent measurements at each time point. ($p \leq 0.05$, **: $p \leq 0.01$, ***: $p \leq 0.001$).
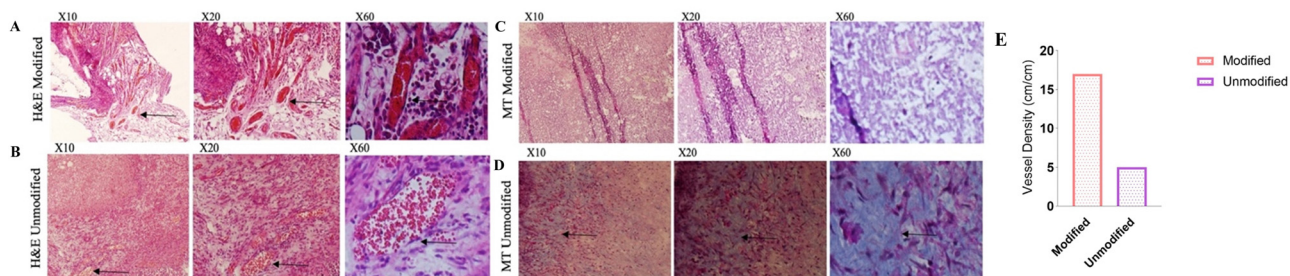
Fig. 6 (A) and (B) Images of hematoxylin and eosin (H&E) and (C) and (D) Masson's trichrome (MT) staining of histological staining of the unmodified and modified microcapsules that were retrieved five weeks post-transplant in the peritoneal cavity. Scale bar: 500 μm. (E) Comparison of vascular density between unmodified and modified microcapsules.

swelling growth is fastest in the first few hours; as time passes, the process slows down and eventually achieves a constant value on the eighth day. The hydration and dehydration characteristics revealed the rate of water penetration, diffusion, and inhibition in the polymer network. K. Baysal *et al.* investigated the swelling behavior of alginate hydrogel with chitosan in their research. According to the findings of this research, which are consistent with our findings, the rate of swelling in 1% alginate is greater than in 3% alginate, and the rate of swelling rises in the first 190 minutes before decreasing until collapse.[66]

In vitro oxygen release of PFOB in the PFOB-laden alginate hydrogel was studied using two methods: an ABG device and a $[Ru(dpp)_3]Cl_2$ fluorescent probe. According to the findings, oxygen emission occurs immediately and continues until the solution saturates or the reaction is completed. Chin K. *et al.* evaluated the metabolic activity of $HepG_2$ cells immobilized in PFOB-laden alginate hydrogel and alginate hydrogel. The findings showed that PFOB-laden alginate hydrogel had increased metabolic activity, demonstrating the relevance of PFOB in metabolic activity.[67] In line with this finding, Liu and colleagues investigated the

oxygen release of H_2O_2/MnO_2 using the $[Ru(dpp)_3]Cl_2$ fluorescent probe. They, too, detected a reduction in the fluorescence emission spectra at 610 nm, suggesting oxygen generation.[68] In the following, the biocompatibility of the macrocapsule reservoir (PFOB-containing alginate hydrogel) was assessed. The findings showed no toxicity, which is also consistent with the earlier PFC research. Maillard *et al.* measured the number of beta cells in the presence of PFOB emulsion and found that it was higher than in the control group.[69]

Hydrogen peroxide, calcium bicarbonate and sodium bicarbonate are the most widely studied oxygen-producing biomaterials. The immediate release of oxygen and the formation of free radicals is one of the drawbacks of these biomaterials. Therefore, these biomaterials require more engineering to prevent possible damage.[54,70] In order to minimize the cytotoxic effects of the hydrogen peroxide, catalase is added to the hydrogel that encapsulates the cells.[70]

Intraperitoneal transplantation of macrocapsules carrying pancreatic islets in C57BL/6 mice showed a significant improvement in the restoration of normoglycemia in diabetic mice without any immunosuppressive treatment for at least 35 days. By analyzing the presented data in Fig. 5B, notable insights can be drawn regarding FBG levels across different groups. The group treated with the macrodevice (islet/Alg/PFOB) shows a falling FBG level starting on day 15 post-transplantation. This decline is of great significance as it effectively brings their levels within the normal range, mirroring those observed in the healthy group. This substantial decrease persists until the study concludes at day 35. Conversely, other groups do not show significant declines in FBG levels. Apart from the group equipped with the macrodevice (Alg > free islet), which displays a minor drop to 250 mg dL^{-1}. This result can be solid evidence that the presence of PFOB in the macrodevice played a pivotal role in enhancing oxygen supply to the transplanted islets. This continuous and ample oxygen supply critically promotes the survival and functionality of these cells. The correlation between employing complete macrodevices (islet/Alg/PFOB) and observing declining FBG levels within the normal range suggests that combining PFOB with islet cells and alginate contributes substantially to the successful transplantation and functioning of these cells. These findings underscore that only mice receiving complete macrodevices effectively regulate their FBG levels compared to other groups, particularly those with solely transplanted islets. Furthermore, PFOB enhances the overall performance and longevity of the transplanted islets significantly. Fig. 5C, portraying blood glucose tolerance monitoring data, also reveals similar trends when mice are treated with different approaches. Specifically, mice treated with the macrodevice (islet/Alg/PFOB) display a pattern akin to healthy ones. Initially, there is a slight increase in blood glucose levels, followed by subsequent decreases that stabilize over time. These findings suggest that utilizing a complete macrodevice proves more efficacious in achieving regulation of blood glucose levels compared to solely relying on islet transplantation alone, which shows limited improvement results. It's significant to note that although PFOB contributes towards

delivering oxygen efficiently, other elements intrinsic to the microdevice, such as its physical structure, composition, and overall functionality, could potentially exert an influential effect. These aspects may also play a pivotal role in successful islet cell transplantation and the regulation of blood glucose levels. Our research findings align with other investigations that highlight the significance of oxygen supply. For instance, in studies involving rat pancreas during digestion, scientists introduced PFC, leading to a gas oxygen pressure of 300 mmHg in the tissues that received it.[71–73] In contrast, tissues without PFC showed no increase in oxygen pressure. Another research investigation revealed that administering exogenous oxygen *via* a gas chamber proved beneficial in preserving normal fasting blood glucose levels for transplanted rats over a span of 7 months.[59] However, it is important to note that maximal oxygen pressure does not necessarily guarantee survival or optimal function of pancreatic islets. Creating optimal conditions remains crucial for both survival and optimal function. In addition to animal studies, researchers have also examined the impact of PFCs on yeasts and fungi. Notably, the introduction of PFC resulted in growth enhancements in *Rhizopus nigricans* and *Saccharomyces cerevisiae* yeast.[56]

The partition coefficient of PFOB is 6.37; therefore, to stabilize it in an aqueous environment such as a hydrogel, the use of a surfactant is inevitable, and due to its biocompatibility, F68 was used as a surfactant in this study.[74] The results of the zeta potential, which is a negative number (-108 mV), confirm its good stability, as a zeta potential greater than ± 30 mV is considered as a general rule of emulsion stability, and the 35 days of oxygenation is probably due to its high stability.[75]

The histopathological test is represented in Fig. 6. Hematoxylin and eosin (H&E) staining was utilized to visualize the vascularization amount in the macrodevice. In Fig. 6A, the modified macrodevice surface with PEG is shown. The presence of vascular sprouts (indicated by arrows) on the modified macrodevice suggests successful vascularization and the establishment of functional blood vessels. This desirable outcome indicates that the use of PEG coating on the modified macrodevice promotes both the growth and integration of blood vessels, ultimately facilitating sufficient blood supply to the surrounding tissues. In contrast, when observing Fig. 6B, which represents the unmodified macrodevice, significant vascular sprouts are not observed. This lack of vascularization indicates a limited degree of blood vessel formation within the unmodified macrodevice. It is worth noting that Fig. 6C and D provides a comparison between MT compression on both the modified macrodevice with a PEG coating and the unmodified macrodevice. Highlighting this comparison are arrows pointing toward fibroid formations seen on the unmodified macrodevice surface. Such formations are considered undesirable, as fibroids are abnormal growths of fibrous tissue that impede proper tissue integration and functionality. The presence of these fibroids suggests that utilizing an unmodified macrodevice may trigger an undesired foreign body response or promote fibrous tissue overgrowth, ultimately hindering overall device performance. On a positive note, when examining Fig. 6C and D for the modified

macrodevice with PEG coating, noteworthy fibroid formations are not observed as depicted in these images. The histopathological findings obtained from this investigation strongly support the idea that PEG surface modification significantly improves both the functionality and biocompatibility characteristics of the macrodevice. Additionally, it encourages positive tissue integration and vascularization while simultaneously mitigating undesired fibroid formations. In line with our study, the investigation also revealed the absence of a fibrous layer surrounding the implanted device. This outcome holds significant importance for the success of transplantation, reflecting the efficacy of altering our surface characteristics.[27] Nevertheless, it is essential to acknowledge certain limitations when employing a macrocapsule for sustained drug delivery purposes. One such setback involves difficulties in loading sufficient levels of an oxygen vector onto its surface, which may hinder proper angiogenesis rates across the membrane's cross sections.

5. Conclusion

The challenge of delivering sufficient amounts of oxygen under hypoxic conditions within a designed macrocapsule is a significant roadblock that researchers have attempted to address in this recent study. The use of a PFOB carrier proved to be an ideal solution for transporting oxygen adequately, while being biocompatible.

Our results showed that the incorporation of PFOB-loaded alginate hydrogel helped to preserve islets during hypoxia exposure and resulted in lower blood glucose levels compared to other study groups that received either macrocapsules (islet/Alg) or free islets for more than 30 days. Moreover, surface modification with PEG polymer helped minimize fibrous capsule formation and prevented any protein absorption on the surface of the modified macrocapsules. Also, we observed sprouting blood vessel formation over the modified-macrocapsule when evaluated immunohistochemically through H&E images. Notably, if retrieved after an extended period, we anticipate that vascular density will increase, leading to even better support for optimal oxygenation needs.

In conclusion, this study highlights the importance of vascularization, preventing protein absorption and fibrosis formation on the surface of macrocapsules, and effective means for oxygen delivery, which are imperative for successful implant device performance.

The findings of this study offer strong evidence that designing macrocapsules with these features can have the potential to be a groundbreaking method for treating diabetes. Additional research and improvements in the design and implementation of the device may lead to its successful use in clinical settings, offering benefits to patients with diabetes.

Disclosure instructions

During the preparation of this work, the authors did not use any generative AI or AI-assisted technologies.

Ethics statement

Author contributions

Z. I. and G. M. designed the study. N. K. performed most of the experiments and wrote the manuscript. Z. I. G. M. and A. A. supervised the project, interpreted the data, provided financial and administrative support, discussed the results, and approved the manuscript. R. M. assisted with the islet isolation process and transplanted the macrocapsule.

Data availability

The data supporting this article have been included as part of the ESI.†

Conflicts of interest

The authors declare no conflict of interest.

Acknowledgements

References

1 B. O. Roep, S. Thomaidou, R. van Tienhoven and A. Zaldumbide, Type 1 diabetes mellitus as a disease of the β-cell (do not blame the immune system?), *Nat. Rev. Endocrinol.*, 2021, **17**(3), 150–161.

2 N. G. Vallianou, T. Stratigou, E. Geladari, C. M. Tessier, C. S. Mantzoros and M. Dalamaga, Diabetes type 1: can it be treated as an autoimmune disorder?, *Rev. Endocr. Metab. Disord.*, 2021, 1–18.

3 M. Neumann, T. Arnould and B.-L. Su, Encapsulation of stem-cell derived β-cells: A promising approach for the treatment for type 1 diabetes mellitus, *J. Colloid Interface Sci.*, 2023, **636**, 90–102.

4 H. Derakhshankhah, S. Sajadimajd, F. Jahanshahi, Z. Samsonchi, H. Karimi, E. Hajizadeh-Saffar, S. Jafari, M. Razmi, S. S. Malvajerd and G. Bahrami, Immunoengineering Biomaterials in Cell-Based Therapy for Type 1 Diabetes, *Tissue Eng., Part B*, 2022, **28**(5), 1053–1066.

5 C. Stabler, Y. Li, J. Stewart and B. Keselowsky, Engineering immunomodulatory biomaterials for type 1 diabetes, *Nat. Rev. Mater.*, 2019, **4**(6), 429–450.

6 A. L. Facklam, L. R. Volpatti and D. G. Anderson, Biomaterials for personalized cell therapy, *Adv. Mater.*, 2020, **32**(13), 1902005.

7 S. Pathak, T. T. Pham, J.-H. Jeong and Y. Byun, Immunoisolation of pancreatic islets via thin-layer surface modification, *J. Controlled Release*, 2019, **305**, 176–193.

8 D. Goswami, D. A. Domingo-Lopez, N. A. Ward, J. R. Millman, G. P. Duffy, E. B. Dolan and E. T. Roche, Design considerations for macroencapsulation devices for stem cell derived islets for the treatment of type 1 diabetes, *Adv. Sci.*, 2021, **8**(16), 2100820.

9 D. An, A. Chiu, J. A. Flanders, W. Song, D. Shou, Y.-C. Lu, L. G. Grunnet, L. Winkel, C. Ingvorsen and N. S. Christophersen, Designing a retrievable and scalable cell encapsulation device for potential treatment of type 1 diabetes, *Proc. Natl. Acad. Sci. U. S. A.*, 2018, **115**(2), E263–E272.

10 D. Dufrane and P. Gianello, Macro-or microencapsulation of pig islets to cure type 1 diabetes, *World J. Gastroenterol.*, 2012, **18**(47), 6885.

11 A. Espona-Noguera, J. Ciriza, A. Cañibano-Hernández, G. Orive, R. M. Hernández, L. Saenz del Burgo and J. L. Pedraz, Review of advanced hydrogel-based cell encapsulation systems for insulin delivery in type 1 diabetes mellitus, *Pharmaceutics*, 2019, **11**(11), 597.

12 M. Kumagai-Braesch, S. Jacobson, H. Mori, X. Jia, T. Takahashi, A. Wernerson, M. Flodström-Tullberg and A. Tibell, The TheraCyte™ device protects against islet allograft rejection in immunized hosts, *Cell Transplant.*, 2013, **22**(7), 1137–1146.

13 B. Cooper-Jones and C. Ford, *Islet cell replacement therapy for insulin-dependent diabetes*, *CADTH Issues in Emerging Health Technologies*, 2017.

14 E. Dolgin, Diabetes cell therapies take evasive action, *Nat. Biotechnol.*, 2022, **40**, 291–295.

15 U. Barkai, A. Rotem and P. de Vos, Survival of encapsulated islets: More than a membrane story, *World J. Transplant.*, 2016, **6**(1), 69.

16 D. An, Y. Ji, A. Chiu, Y.-C. Lu, W. Song, L. Zhai, L. Qi, D. Luo and M. Ma, Developing robust, hydrogel-based, nanofiber-enabled encapsulation devices (NEEDs) for cell therapies, *Biomaterials*, 2015, **37**, 40–48.

17 L. Fath-Bayati and J. Ai, Assessment of mesenchymal stem cell effect on foreign body response induced by intraperitoneally implanted alginate spheres, *J. Biomed. Mater. Res., Part A*, 2020, **108**(1), 94–102.

18 D. Eleftheriadou, R. E. Evans, E. Atkinson, A. Abdalla, F. K. Gavins, A. S. Boyd, G. R. Williams, J. C. Knowles, V. H. Roberton and J. B. Phillips, An alginate-based encapsulation system for delivery of therapeutic cells to the CNS, *RSC Adv.*, 2022, **12**(7), 4005–4015.

19 J. S. Caserto, D. T. Bowers, K. Shariati and M. Ma, Biomaterial Applications in Islet Encapsulation and Transplantation, *ACS Appl. Bio Mater.*, 2020, **3**(12), 8127–8135.

20 Z. Samsonchi, H. Karimi, Z. Izadi, P. Baei, M. Najarasl, M. K. Ashtiani, J. Mohammadi, M. Moazenchi, Y. Tahamtani and H. Baharvand, Transplantation of Islet-Containing microcapsules modified with constitutional isomers of sulfated alginate in diabetic mice to mitigate fibrosis for Long-term glycemic control, *Chem. Eng. J.*, 2022, **432**, 134298.

21 P.-J. Huang, J. Qu, P. Saha, A. Muliana and J. Kameoka, Microencapsulation of beta cells in collagen micro-disks via circular pneumatically actuated soft micro-mold (cPASMO) device, *Biomed. Phys. Eng. Express*, 2018, **5**(1), 015004.

22 C. H. Stephens, R. A. Morrison, M. McLaughlin, K. Orr, S. A. Tersey, J. C. Scott-Moncrieff, R. G. Mirmira, R. V. Considine and S. Voytik-Harbin, Oligomeric collagen as an encapsulation material for islet/β-cell replacement: Effect of islet source, dose, implant site, and administration format, *Am. J. Physiol.: Endocrinol. Metab.*, 2020, **319**(2), E388–E400.

23 T. Qin, S. Hu and P. de Vos, A composite capsule strategy to support longevity of microencapsulated pancreatic β cells, *Biomater. Adv.*, 2023, **155**, 213678.

24 T. Boettler, D. Schneider, Y. Cheng, K. Kadoya, E. P. Brandon, L. Martinson and M. Von Herrath, Pancreatic tissue transplanted in TheraCyte™ encapsulation devices is protected and prevents hyperglycemia in a mouse model of immune-mediated diabetes, *Cell Transplant.*, 2016, **25**(3), 609–614.

25 A. Mora-Boza, L. M. M. Castro, R. S. Schneider, W. M. Han, A. J. García, B. Vázquez-Lasa and J. San Román, Microfluidics generation of chitosan microgels containing glyceryl-phytate crosslinker for in situ human mesenchymal stem cells encapsulation, *Mater. Sci. Eng., C*, 2021, **120**, 111716.

26 G. Michielin and S. J. Maerkl, Direct encapsulation of biomolecules in semi-permeable microcapsules produced with double-emulsions, *Sci. Rep.*, 2022, **12**(1), 1–9.

27 K. Skrzypek, M. Groot Nibbelink, J. Van Lente, M. Buitinga, M. A. Engelse, E. J. De Koning, M. Karperien, A. Van Apeldoorn and D. Stamatialis, Pancreatic islet macroencapsulation using microwell porous membranes, *Sci. Rep.*, 2017, **7**(1), 1–12.

28 R. P. Tan, N. Hallahan, E. Kosobrodova, P. L. Michael, F. Wei, M. Santos, Y. T. Lam, A. H. Chan, Y. Xiao and M. M. Bilek, Bioactivation of encapsulation membranes reduces fibrosis and enhances cell survival, *ACS Appl. Mater. Interfaces*, 2020, **12**(51), 56908–56923.

29 B. Kupikowska-Stobba, D. Lewińska and M. Grzeczkowicz, Chemical method for retrieval of cells encapsulated in alginate-polyethersulfone microcapsules, *Artif. Cells, Nanomed., Biotechnol.*, 2014, **42**(3), 151–160.

30 A. M. Smink, K. Skrzypek, J. A. Liefers-Visser, R. Kuwabara, B. J. De Haan, P. De Vos and D. Stamatialis, In vivo vascularization and islet function in a microwell device for pancreatic islet transplantation, *Biomed. Mater.*, 2021, **16**(3), 035036.

31 M. He, Q. Wang, R. Wang, Y. Xie, W. Zhao and C. Zhao, Design of antibacterial poly (ether sulfone) membranes via

covalently attaching hydrogel thin layers loaded with Ag nanoparticles, *ACS Appl. Mater. Interfaces*, 2017, **9**(19), 15962–15974.

32 K. Skrzypek, M. G. Nibbelink, L. P. Karbaat, M. Karperien, A. van Apeldoorn and D. Stamatialis, An important step towards a prevascularized islet macroencapsulation device—effect of micropatterned membranes on development of endothelial cell network, *J. Mater. Sci.: Mater. Med.*, 2018, **29**(7), 1–15.

33 M. Cao, G. Wang, H. He, R. Yue, Y. Zhao, L. Pan, W. Huang, Y. Guo, T. Yin and L. Ma, Hemoglobin-based oxygen carriers: potential applications in solid organ preservation, *Front. Pharmacol.*, 2021, **12**, 760215.

34 N. Mohanto, Y.-J. Park and J.-P. Jee, Current perspectives of artificial oxygen carriers as red blood cell substitutes: a review of old to cutting-edge technologies using *in vitro* and *in vivo* assessments, *J. Pharm. Invest.*, 2023, **53**(1), 153–190.

35 A. Stefanek, A. Kulikowska-Darłak, K. Bogaj, A. Nowak, J. Dembska and T. Ciach, Biomimetic alginate/perfluorocarbon microcapsules–the effect on in vitro metabolic activity and long-term cell culture, *Chem. Process Eng.*, 2022, 81–95.

36 S. A. Fernandez, L. Danielczak, G. Gauvin-Rossignol, C. Hasilo, A. Bégin-Drolet, J. Ruel, S. Paraskevas, R. L. Leask and C. A. Hoesli, An in vitro Perfused Macroencapsulation Device to Study Hemocompatibility and Survival of Islet-Like Cell Clusters, *Front. Bioeng. Biotechnol.*, 2021, **9**, 674125.

37 A. R. Pepper, B. Gala-Lopez, R. Pawlick, S. Merani, T. Kin and A. Shapiro, A prevascularized subcutaneous device-less site for islet and cellular transplantation, *Nat. Biotechnol.*, 2015, **33**(5), 518–523.

38 L. Nalbach, L. P. Roma, B. M. Schmitt, V. Becker, C. Körbel, S. Wrublewsky, M. Pack, T. Später, W. Metzger and M. M. Menger, Improvement of islet transplantation by the fusion of islet cells with functional blood vessels, *EMBO Mol. Med.*, 2021, **13**(1), e12616.

39 A. Kale and N. M. Rogers, No Time to Die—How Islets Meet Their Demise in Transplantation, *Cells*, 2023, **12**(5), 796.

40 L. Montazeri, S. Hojjati-Emami, S. Bonakdar, Y. Tahamtani, E. Hajizadeh-Saffar, M. Noori-Keshtkar, M. Najar-Asl, M. K. Ashtiani and H. Baharvand, Improvement of islet engrafts by enhanced angiogenesis and microparticle-mediated oxygenation, *Biomaterials*, 2016, **89**, 157–165.

41 J.-P. Liang, R. P. Accolla, M. Soundirarajan, A. Emerson, M. M. Coronel and C. L. Stabler, Engineering a macroporous oxygen-generating scaffold for enhancing islet cell transplantation within an extrahepatic site, *Acta Biomater.*, 2021, **130**, 268–280.

42 M. Rafique, O. Ali, M. Shafiq, M. Yao, K. Wang, H. Ijima, D. Kong and M. Ikeda, Insight on Oxygen-Supplying Biomaterials Used to Enhance Cell Survival, Retention, and Engraftment for Tissue Repair, *Biomedicines*, 2023, **11**(6), 1592.

43 E. Lambert, V. S. Gorantla and J. M. Janjic, Pharmaceutical design and development of perfluorocarbon nanocolloids for oxygen delivery in regenerative medicine, *Nanomedicine*, 2019, **14**(20), 2697–2712.

44 A. Rodriguez-Brotons, W. Bietiger, C. Peronet, A. Langlois, J. Magisson, C. Mura, C. Sookhareea, V. Polard, N. Jeandidier and F. Zal, Comparison of perfluorodecalin and HEMOXCell as oxygen carriers for islet oxygenation in an in vitro model of encapsulation, *Tissue Eng., Part A*, 2016, **22**(23–24), 1327–1336.

45 H. Brandhorst, B. Theisinger, H. Yamaya, J. Henriksnäs, P. O. Carlsson, O. Korsgren and D. Brandhorst, Perfluorohexyloctane improves long-term storage of rat pancreata for subsequent islet isolation, *Transplant Int.*, 2009, **22**(10), 1017–1022.

46 C. A. Fraker, S. Cechin, S. Álvarez-Cubela, F. Echeverri, A. Bernal, R. Poo, C. Ricordi, L. Inverardi and J. Domínguez-Bendala, A physiological pattern of oxygenation using perfluorocarbon-based culture devices maximizes pancreatic islet viability and enhances β-cell function, *Cell Transplant.*, 2013, **22**(9), 1723–1733.

47 S. H. Lee, H. S. Park, Y. Yang, E. Y. Lee, J. W. Kim, G. Khang and K. H. Yoon, Improvement of islet function and survival by integration of perfluorodecalin into microcapsules in vivo and in vitro, *J. Tissue Eng. Regener. Med.*, 2018, **12**(4), e2110–e2122.

48 S. Suvarnapathaki, X. Wu, D. Lantigua, M. A. Nguyen and G. Camci-Unal, Breathing life into engineered tissues using oxygen-releasing biomaterials, *NPG Asia Mater.*, 2019, **11**(1), 65.

49 E. Hajizadeh-Saffar, Y. Tahamtani, N. Aghdami, K. Azadmanesh, M. Habibi-Anbouhi, Y. Heremans, N. De Leu, H. Heimberg, P. Ravassard and M. Shokrgozar, Inducible VEGF expression by human embryonic stem cell-derived mesenchymal stromal cells reduces the minimal islet mass required to reverse diabetes, *Sci. Rep.*, 2015, **5**(1), 1–10.

50 Z. Izadi, E. Hajizadeh-Saffar, J. Hadjati, M. Habibi-Anbouhi, M. H. Ghanian, H. Sadeghi-Abandansari, M. K. Ashtiani, Z. Samsonchi, M. Raoufi and M. Moazenchi, Tolerance induction by surface immobilization of Jagged-1 for immunoprotection of pancreatic islets, *Biomaterials*, 2018, **182**, 191–201.

51 F. Sun, J. Yang, Q. Shen, M. Li, H. Du and D. Y. Xing, Conductive polyethersulfone membrane facilely prepared by simultaneous phase inversion method for enhanced antifouling and separation under low driven-pressure, *J. Environ. Manage.*, 2021, **297**, 113363.

52 J. Garcia-Ivars, M.-I. Iborra-Clar, M.-I. Alcaina-Miranda, J.-A. Mendoza-Roca and L. Pastor-Alcañiz, Development of fouling-resistant polyethersulfone ultrafiltration membranes via surface UV photografting with polyethylene glycol/aluminum oxide nanoparticles, *Sep. Purif. Technol.*, 2014, **135**, 88–99.

53 S. Wu, L. Wang, Y. Fang, H. Huang, X. You and J. Wu, Advances in encapsulation and delivery strategies for islet transplantation, *Adv. Healthcare Mater.*, 2021, **10**(20), 2100965.

54 K. K. Papas, H. De Leon, T. M. Suszynski and R. C. Johnson, Oxygenation strategies for encapsulated islet and beta cell transplants, *Adv. Drug Delivery Rev.*, 2019, **139**, 139–156.

55 R. Augustine, M. Gezek, N. S. Bostanci, A. Nguyen and G. Camci-Unal, Oxygen-generating scaffolds: One step closer to the clinical translation of tissue engineered products, *Chem. Eng. J.*, 2023, **455**, 140783.

56 H. Komatsu, F. Kandeel and Y. Mullen, Impact of oxygen on pancreatic islet survival, *Pancreas*, 2018, **47**(5), 533.

57 R. Cao, E. Avgoustiniatos, K. Papas, P. de Vos and J. R. Lakey, Mathematical predictions of oxygen availability in micro-and macro-encapsulated human and porcine pancreatic islets, *J. Biomed. Mater. Res., Part B*, 2020, **108**(2), 343–352.

58 N. Kakaei, R. Amirian, M. Azadi, G. Mohammadi and Z. Izadi, Perfluorocarbons: A perspective of theranostic applications and challenges, *Front. Bioeng. Biotechnol.*, 2023, **11**, 1115254.

59 Y. Evron, C. K. Colton, B. Ludwig, G. C. Weir, B. Zimermann, S. Maimon, T. Neufeld, N. Shalev, T. Goldman and A. Leon, Long-term viability and function of transplanted islets macroencapsulated at high density are achieved by enhanced oxygen supply, *Sci. Rep.*, 2018, **8**(1), 1–13.

60 J. Prince, S. Bhuvana, K. Boodhoo, V. Anbharasi and G. Singh, Synthesis and characterization of PEG-Ag immobilized PES hollow fiber ultrafiltration membranes with long lasting antifouling properties, *J. Membr. Sci.*, 2014, **454**, 538–548.

61 J. Peng, Y. Su, Q. Shi, W. Chen and Z. Jiang, Protein fouling resistant membrane prepared by amphiphilic pegylated polyethersulfone, *Bioresour. Technol.*, 2011, **102**(3), 2289–2295.

62 Y. Du, X. Chen, Y. Mou, L. Chen, X. Li, J. Wang, Y. Shu, Y. Zhao and N. Huang, Improving hemocompatibility and antifouling performance of polyethersulfone membrane by in situ incorporation of phosphorylcholine polymers, *Appl. Surf. Sci.*, 2024, 159646.

63 A. Abdelrasoul and A. Shoker, Induced hemocompatibility of polyethersulfone (PES) hemodialysis membrane using polyvinylpyrrolidone: Investigation on human serum fibrinogen adsorption and inflammatory biomarkers released, *Chem. Eng. Res. Des.*, 2022, **177**, 615–624.

64 A. Modi, S. K. Verma and J. Bellare, Surface-functionalized poly (ether sulfone) composite hollow fiber membranes with improved biocompatibility and uremic toxins clearance for bioartificial kidney application, *ACS Appl. Bio Mater.*, 2020, **3**(3), 1589–1597.

65 B. K. Moghadas, A. Akbarzadeh, M. Azadi, A. Aghili, A. S. Rad and S. Hallajian, The morphological properties and biocompatibility studies of synthesized nanocomposite foam from modified polyethersulfone/graphene oxide using supercritical CO_2, *J. Macromol. Sci., Part A: Pure Appl.Chem.*, 2020, **57**(6), 451–460.

66 K. Baysal, A. Z. Aroguz, Z. Adiguzel and B. M. Baysal, Chitosan/alginate crosslinked hydrogels: Preparation, characterization and application for cell growth purposes, *Int. J. Biol. Macromol.*, 2013, **59**, 342–348.

67 K. Chin, S. F. Khattak, S. R. Bhatia and S. C. Roberts, Hydrogel-perfluorocarbon composite scaffold promotes oxygen transport to immobilized cells, *Biotechnol. Prog.*, 2008, **24**(2), 358–366.

68 J. Liu, W. Zhang, A. Kumar, X. Rong, W. Yang, H. Chen, J. Xie and Y. Wang, Acridine orange encapsulated mesoporous manganese dioxide nanoparticles to enhance radiotherapy, *Bioconjugate Chem.*, 2019, **31**(1), 82–92.

69 E. Maillard, M. Juszczak, A. Langlois, C. Kleiss, M. Sencier, W. Bietiger, M. Sanchez-Dominguez, M. Krafft, P. Johnson and M. Pinget, Perfluorocarbon emulsions prevent hypoxia of pancreatic β-cells, *Cell Transplant.*, 2012, **21**(4), 657–669.

70 M. S. Toftdal, N. Taebnia, F. B. Kadumudi, T. L. Andresen, T. Frogne, L. Winkel, L. G. Grunnet and A. Dolatshahi-Pirouz, Oxygen releasing hydrogels for beta cell assisted therapy, *Int. J. Pharm.*, 2021, **602**, 120595.

71 T. Kin, M. Mirbolooki, P. Salehi, M. Tsukada, D. O'Gorman, S. Imes, E. A. Ryan, A. M. J. Shapiro and J. R. Lakey, Islet isolation and transplantation outcomes of pancreas preserved with University of Wisconsin solution versus two-layer method using preoxygenated perfluorocarbon, *Transplantation*, 2006, **82**(10), 1286–1290.

72 E. Ortiz-Prado, J. F. Dunn, J. Vasconez, D. Castillo and G. Viscor, Partial pressure of oxygen in the human body: a general review, *Am. J. Blood Res.*, 2019, **9**(1), 1.

73 M. P. Krafft and J. G. Riess, Therapeutic oxygen delivery by perfluorocarbon-based colloids, *Adv. Colloid Interface Sci.*, 2021, **294**, 102407.

74 J. C. White, *Strategies for improving oxygen transport and mechanical strength in alginate-based hydrogels*, University of Massachusetts Amherst, 2014.

75 Z. Németh, I. Csóka, R. Semnani Jazani, B. Sipos, H. Haspel, G. Kozma, Z. Kónya and D. G. Dobó, Quality by design-driven zeta potential optimisation study of liposomes with charge imparting membrane additives, *Pharmaceutics*, 2022, **14**(9), 1798.